Valence band structure of the Si(331)-(12 × 1) surface reconstruction

2011 J. Phys.: Condens. Matter 23 135003

(http://iopscience.iop.org/0953-8984/23/13/135003)

IOP Publishing Journal of Physics: Condensed Matter

J. Phys.: Condens. Matter **23** (2011) 135003 (5pp) doi:10.1088/0953-8984/23/13/135003

Valence band structure of the Si(331)-(12 × 1) surface reconstruction

Corsin Battaglia[1], Eike Fabian Schwier[2], Claude Monney[2,4], Clément Didiot[2], Nicolas Mariotti[2], Katalin Gaál-Nagy[3,5], Giovanni Onida[3], Michael Gunnar Garnier[2] and Philipp Aebi[2]

[1] Ecole Polytechnique Fédérale de Lausanne (EPFL), Institute of Microengineering (IMT), Photovoltaics and Thin Film Electronics Laboratory, Rue A-L Breguet 2, 2000 Neuchâtel, Switzerland

[2] Department of Physics and Fribourg Center for Nanomaterials, Université de Fribourg, Chemin du Musée 3, 1700 Fribourg, Switzerland

[3] Dipartimento di Fisica and European Theoretical Spectroscopy Facility (ETSF), Università degli Studi di Milano, Via Celoria 16, 20133 Milano, Italy

E-mail: corsin.battaglia@epfl.ch

Received 26 December 2010, in final form 31 January 2011
Published 14 March 2011
Online at stacks.iop.org/JPhysCM/23/135003

Abstract

Using angle-resolved photoelectron spectroscopy we investigate the electronic valence band structure of the Si(331)-(12 × 1) surface reconstruction for which we recently proposed a structural model containing silicon pentamers as elementary structural building blocks. We find that this surface, reported to be metallic in a previous study, shows a clear band gap at the Fermi energy, indicating semiconducting behavior. An occupied surface state, presumably containing several spectral components, is found centered at −0.6 eV exhibiting a flat energy dispersion. These results are confirmed by scanning tunneling spectroscopy and are consistent with recent first-principles calculations for our structural model.

1. Introduction

Understanding the interplay between the structural and electronic properties of silicon surfaces is interesting not only from a fundamental point of view but it becomes increasingly important for technological applications. Previous angle-resolved photoelectron spectroscopy (ARPES) studies focused on the valence band structure of the Si(100)-c(4 × 2) [1–3], Si(111)-(7 × 7) [4–7] and Si(110)-(16 × 2) [8–10] surface reconstructions and their relation to the atomic structure [11].

Here we report for the first time ARPES results for the Si(331)-(12 × 1) surface reconstruction. Si(331) is of particular importance because it is the only planar silicon surface with a stable reconstruction located between the (111) and (110) directions. Since its discovery 20 years ago [12] several structural models containing dimers and adatoms as elementary structural building blocks have been proposed [13, 14]. We recently revealed the presence of an additional building block on the Si(331)-(12 × 1) surface. Using scanning tunneling microscopy (STM) we were able to resolve for the first time rows of pentagon pairs running across the Si(331) surface [15]. Inspired by the adatom–tetramer-interstitial (ATI) model for the Si(110)-(16 × 2) surface [16, 17], we proposed a structural model containing silicon pentamers and adatoms as elementary structural building blocks [11, 15].

So far the electronic structure of the Si(331)-(12 × 1) reconstruction has not yet been investigated in detail. Based on the fact that they were able to image the Si(331) surface with an STM bias of ±50 meV or lower, Gai *et al* [14] concluded that the surface must be metallic in nature. In contrast to the metallic behavior reported by Gai *et al*, our valence band spectra obtained from ARPES unambiguously reveal a band gap indicating semiconducting behavior and a flat, almost non-dispersing, surface state at −0.6 eV. This result is confirmed by scanning tunneling spectroscopy (STS) and is consistent with first-principles calculations for our structural model.

2. Experiment

Experiments were carried out on boron doped Si(331) samples from Crystec with a resistivity of 0.1–30 Ω cm. Preparation

[4] Present address: Paul Scherrer Institut, Research Department Synchrotron Radiation and Nanotechnology, 5232 Villigen, Switzerland.

[5] Present address: Via Monte Velino 17, 20137 Milano, Italy.

of high quality, atomically precise Si(331)-(12 × 1) surfaces was described in detail in [18]. Experiments were performed in an ultra-high vacuum chamber with a residual gas pressure below 3×10^{-11} mbar equipped with an upgraded Scienta SES-200 hemispherical analyzer with energy and angular resolution set to 20 meV and 0.5°, respectively. Monochromatized, p-polarized He I photons of energy 21.218 eV were used for all measurements. The Fermi energy was calibrated by measuring polycrystalline molybdenum from the Si(331) sample holder. Samples were oriented using an Omicron low-energy electron diffraction (LEED) setup. STM experiments were carried out using an Omicron low-temperature STM. All measurements were performed at room temperature unless otherwise stated. Details of the calculations performed within first-principles density functional theory were given in [19].

3. Results and discussion

Before presenting our experimental ARPES band maps, we briefly review the geometry of the Si(331) surface. Figure 1(a) presents an experimental STM image showing the double rows of silicon pentamers running along the $[\bar{1}\bar{1}6]$ direction. The orientation of the surface with respect to the bulk is indicated along with the unit cell of the (12 × 1) surface reconstruction (dashed rectangle). The various features observed in the STM image were discussed in detail in [15]. In figure 1(b) we present the relationship between the real space Bravais lattice and the reciprocal space of the Si(331) surface. The unit cell in real space and the Brillouin zone in reciprocal space for the unreconstructed bulk-terminated (1× 1) symmetry of the Si(331) surface are drawn as continuous lines; the corresponding entities for the reconstructed (12 × 1) surface supercell are drawn as dashed lines. Although conventionally called the (12 × 1) reconstruction, because of the 11 satellite diffraction spots in between the integer spots along the $[\bar{1}10]$ direction observed in LEED patterns [15], the surface supercell is more correctly described in matrix notation by

$$\begin{pmatrix} \mathbf{A}_1 \\ \mathbf{A}_2 \end{pmatrix} = \begin{pmatrix} 2 & 1 \\ 0 & 6 \end{pmatrix} \begin{pmatrix} \mathbf{a}_1 \\ \mathbf{a}_2 \end{pmatrix}.$$

Note also the shaded gray areas within the (12 × 1) unit cells of figure 1(b), which indicate the glide plane symmetry in real space, which reduces to a mirror symmetry in reciprocal space as discussed in [15].

We now turn to our experimental ARPES data. Figures 2(a) and (b) show photoelectron band maps along the $\bar{\Gamma}\bar{A}$ and $\bar{\Gamma}\bar{B}$ directions (see figure 1(b) for the position of the high symmetry points $\bar{\Gamma}$, $\bar{A}$ and $\bar{B}$ within the surface Brillouin zone). E_F denotes the Fermi energy. Here we reference locations in reciprocal space with respect to the (1 × 1) surface Brillouin zone of the unreconstructed surface as we do not observe a clear modulation in the experimental band structure, which we could associate with the (12 × 1) geometry. The band dispersion along $\bar{\Gamma}\bar{A}$ exhibits approximately a mirror symmetry within the (1 × 1) unit cell with respect to $\bar{\Gamma}$ (slightly broken by the p-polarization of the incident He I photons), but no mirror symmetry is observed along $\bar{\Gamma}\bar{B}$. This can be expected from the symmetry of the bulk-terminated

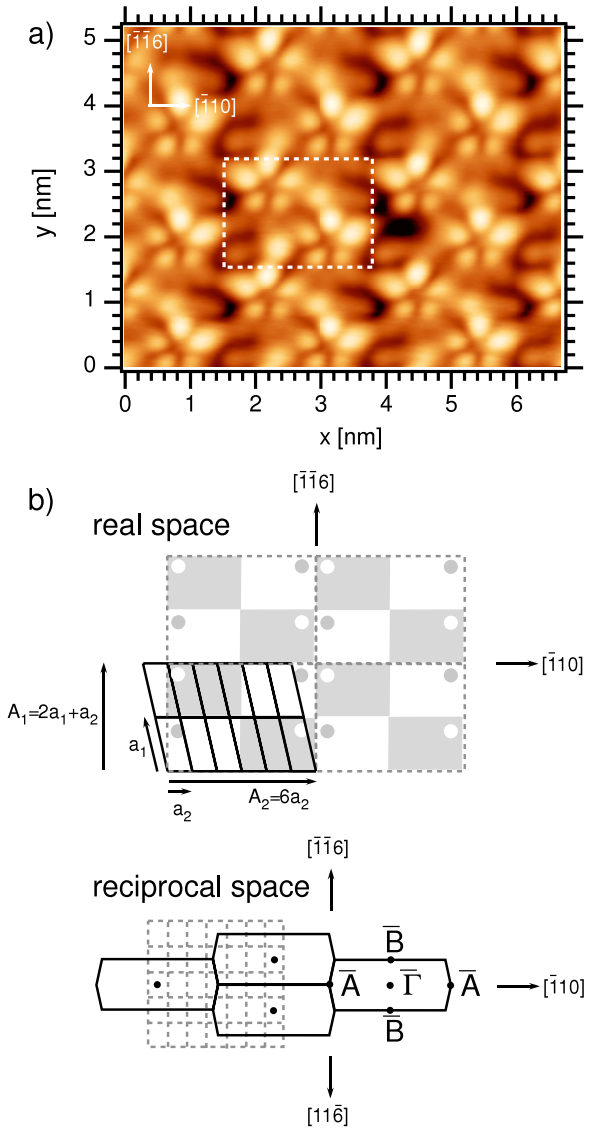

Figure 1. (a) High-resolution STM image with a (12 × 1) unit cell (dashed line) indicated (see text for details of the unit cell). Bias voltage 2.0 V, set-point current 0.06 nA, temperature 77 K. (b) A sketch of the Bravais lattice of the Si(331) surface in real and reciprocal space. The unit cell and Brillouin zone for the (1 × 1) and (12 × 1) symmetries are drawn with continuous and dashed lines, respectively.

(This figure is in colour only in the electronic version)

Si(331) surface (see for example page 5 of [11] for a balls-and-sticks drawing). The solid white lines denote the calculated valence band edge of the silicon bulk band structure projected onto the Si(331) surface, computed within the local density approximation (LDA). The top edge of the valence band was placed at −0.6 eV in order to cover all dispersing bands close to E_F. Besides several strongly dispersing features (band width >2 eV) within the projected bulk band structure, we find a flat, almost non-dispersing, broad band centered at −0.6 eV (band width of peak center <0.2 eV, outlined by gray lines), which we identify as a surface state, since it reaches into the bulk band gap. Close to $\bar{\Gamma}$, this band turns into a surface resonance as it intersects the bulk states (see also the energy

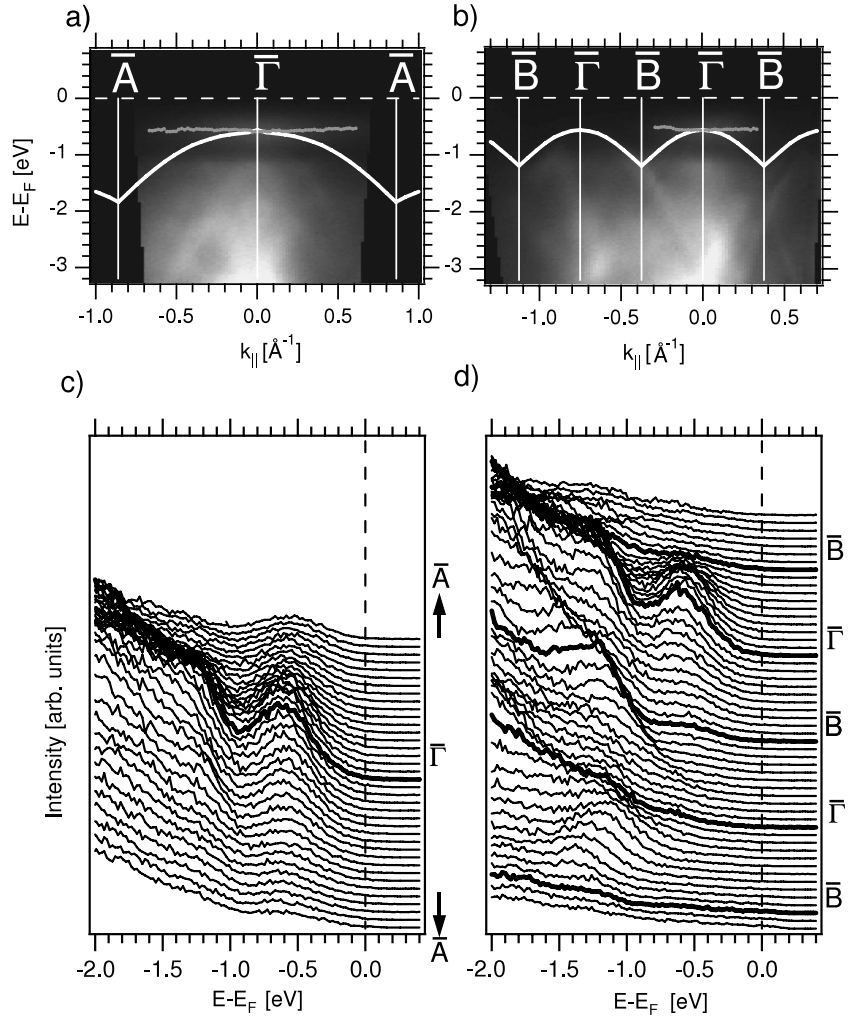

Figure 2. Experimental band dispersion of the Si(331)-(12 × 1) surface. (a) and (b) gray-scale band maps with binding energy E–E_{F} versus parallel momentum $\mathbf{k}_{||}$ along the (1× 1) $\bar{\Gamma}\bar{A}$ and $\bar{\Gamma}\bar{B}$ directions, respectively. The edge of the surface projected bulk band structure is shown by the solid white lines. The fitted positions of the surface state/resonance are indicated by gray lines; (c) and (d) the corresponding energy dispersion curves extracted from the band maps in (a) and (b).

dispersion curves in figures 2(c) and (d) extracted from the band maps in figures 2(a) and (b), respectively). We expect that this surface state contains several spectral components, which reflect the complexity of the atomic structure of this surface reconstruction. In order to investigate further the spectral composition of this state, a detailed study as a function of photon energy would be desirable, allowing us to optimize the ARPES cross section for individual surface states. A surface state of the Si(331)-(12 × 1) reconstruction should exhibit the (12 × 1) periodicity of the surface. However, because of the small size of the (12 × 1) Brillouin zone (see again figure 1(b)) and possibly localized nature of these states, no clear modulation associated with the periodicity of the supercell is observed in the experimental band maps. This can be understood as follows: a single band with a certain bandwidth within the (1 × 1) unit cell will, upon (12 × 1) reconstruction, split into 12 subbands via backfolding at the (12 × 1) Brillouin zone boundaries. The Brillouin zone will therefore be filled with subbands over the previous bandwidth. Thus the many subbands will form a large, seemingly non-dispersing band, where the (12 × 1) periodicity cannot be resolved anymore. This effect is more pronounced the larger/smaller the unit cell/Brillouin zone of the surface reconstruction. In contrast, the bulk bands should exhibit a dominant (1 × 1) periodicity, since they are only very slightly affected by the periodicity of the surface.

Focusing now on the energy dispersion curves in figures 2(c) and (d), in particular on what happens close to the Fermi energy ($E - E_{\mathrm{F}} = 0$), we see that for both directions, no discernible photoelectron intensity is observed. This clearly implies that the surface exhibits semiconducting behavior in contrast to the earlier report by Gai *et al* [14]. In figure 3 we compare the photoemission spectra of Si(331)-(12 × 1) and Si(111)-(7 × 7) measured at normal emission, i.e. for $\bar{\Gamma}$. For comparison we also show a Fermi step measured on polycrystalline molybdenum. Whereas Si(111)-(7 × 7) clearly exhibits a finite spectral intensity at the Fermi energy similar to the molybdenum polycrystal, we see a clear gap for Si(331)-(12 × 1).

In figure 3 we also present a conductance $\mathrm{d}I/\mathrm{d}V$ spectrum obtained via STS by recording the variation of the tunneling current while varying the bias between the sample and the STM

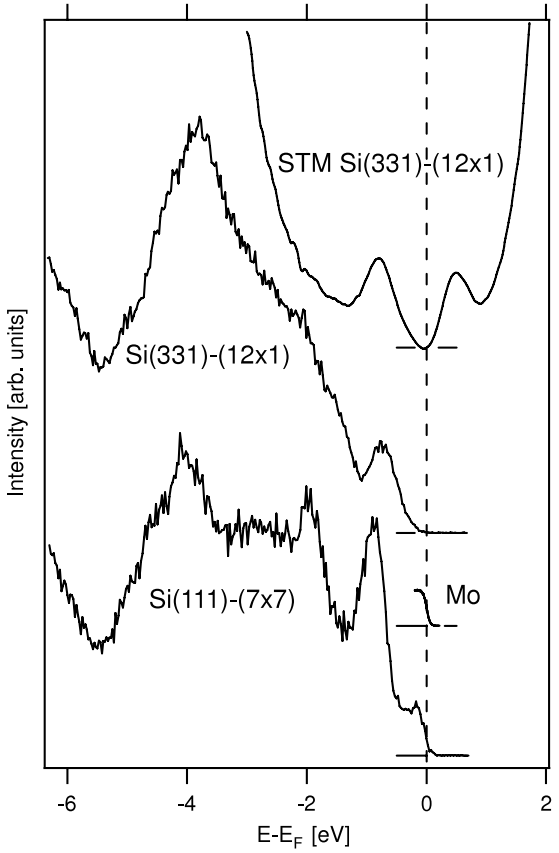

Figure 3. Comparison between the photoemission spectrum of Si(331)-(12 × 1) and Si(111)-(7 × 7) at $\bar{\Gamma}$. For reference purposes a Fermi step measured on polycrystalline Mo is also shown. In addition a dI/dV curve obtained with the STM at room temperature is also shown.

tip. The STS spectrum shows very nice agreement with the ARPES spectrum, in particular, the occupied surface state with a maximum at about −0.6 eV below the Fermi energy is nicely reproduced, although its precise position slightly varies from spectrum to spectrum depending on the location on the surface and on the tip condition. Interestingly, a second clearly defined state is seen exhibiting a maximum at 0.5 eV in the unoccupied part of the spectrum.

From the positions of the two peak maxima we can derive an upper limit for the gap of the Si(331)-(12 × 1) surface of 1.1 eV. Taking into account the broad character of the peaks, a more realistic estimate is obtained by taking the positions of the half-maximum of the two peaks. This gives an estimated value for the gap between 0.5 and 0.6 eV. For a more accurate value a more detailed knowledge of the spectral components of the peaks centered at −0.6 and 0.5 eV is required.

In contrast, the calculated band gap for the structural model we recently proposed for the Si(331)-(12 × 1) surface in [15] is 0.25 eV.[6] However, it is well known that the LDA underestimates the band gap energy of silicon. For bulk silicon we obtain an LDA band gap of 0.55 eV, whereas experimental values are in the range of 1.1–1.2 eV [20] for the temperatures we are interested in here. So the LDA calculation underestimates the bulk band gap by a factor of two. Applying the same factor to the surface calculation yields a theoretical band gap of about 0.5 eV, a value which is consistent with the estimated value of 0.5–0.6 eV derived above from experiment.

It is instructive to compare our ARPES data for Si(331)-(12 × 1) with data reported in the literature for Si(110)-(16 × 2), a surface reconstruction, which we believe shares the same structural building blocks as the Si(331)-(12 × 1) surface, namely pentamers and adatoms. A very similar non-dispersing surface state was observed at −0.4 eV by Kim *et al* [9] in the bulk band gap of the Si(110)-(16 × 2) surface accompanied by a second flat surface state at −0.9 eV. They concluded that these states may be linked to the pentamers and adatoms due to their spatially localized electronic character. Even more recently, Sakamoto *et al* [10] were able to resolve each of these states into two distinct components located at −0.2, −0.4 eV and −0.75, −1.0 eV, respectively. Similar to the Si(331)-(12 × 1) surface reconstruction, the results of both studies indicate semiconducting behavior for the Si(110)-(16 × 2) reconstruction, as no spectral intensity is observed at the Fermi energy. Further investigations will be required to fully understand the link between the structural and electronic properties of these highly complex surface reconstructions.

4. Conclusion

The valence band structure of the Si(331)-(12 × 1) surface reconstruction was investigated by angle-resolved photoelectron spectroscopy. From the ARPES spectra we identify a distinct occupied surface state centered at −0.6 eV, without significant dispersion. However, we cannot exclude that this state is composed of several spectral components. This state is also observed in STS spectra. In addition, using STS we observe a further distinct state at 0.5 eV in the unoccupied part of the spectrum. All experimental spectra are clearly gapped, indicating unambiguous semiconducting behavior in contrast to a previous report. A finite band gap is also consistent with the LDA calculation for the structural model we recently proposed for the Si(331)-(12 × 1) surface reconstruction. Finally, similarities between the band structures of the Si(331)-(12 × 1) reconstruction and the closely related Si(110)-(16 × 2) reconstruction were discussed.

Acknowledgments

Skilful technical assistance was provided by the workshop and electric engineering team of the Université de Neuchâtel. In particular we would like to thank Christian Hêche, Isidro Fernandez, André Cornu and Jean-Pierre Bourquin for the conception and realization of the molybdenum sample holder as well as Daniel Varidel and Urs Bart for their support in improving the measurement electronics. This work was supported by the Fonds National Suisse pour la Recherche Scientifique through Div. II, the Swiss National Center of Competence in Research MaNEP, and by the EU's 7th

[6] The gap value of 0.25 eV is for model T4e in [19]. The gap values for the other models discussed in this paper are 0.03 eV (pentagons only), 0.07 eV (T4 without pentagons), 0.11 eV (T4e without pentagons), 0.10 eV (T4), 0.11 eV (H3), 0.12 eV (A3), 0.22 eV (T4a), 0.14 eV (T4b), 0.07 eV (T4c), 0.07 eV (T4d), 0.23 eV (T4a + b).

Framework Programme through the e-I3 ETSF initiative (Grant Agreement n. 211956).

References

[1] Johansson L S O, Uhrberg R I G, Mårtensson P and Hansson G V 1990 *Phys. Rev.* B **42** 1305
[2] Landemark E, Karlsson C J, Johansson L S O and Uhrberg R I G 1994 *Phys. Rev.* B **49** 16523
[3] Eriksson P E J, Adell M, Sakamoto K and Uhrberg R I G 2008 *Phys. Rev.* B **77** 085406
[4] Himpsel F J, Hollinger G and Pollak R A 1983 *Phys. Rev.* B **28** 7014
[5] Uhrberg R I G, Kaurila T and Chao Y-C 1998 *Phys. Rev.* B **58** R1730
[6] Losio R, Altmann K N and Himpsel F J 2000 *Phys. Rev.* B **61** 10845
[7] Zhang H M, Sakamoto K, Hansson G V and Uhrberg R I G 2008 *Phys. Rev.* B **78** 035318
[8] Cricenti A, Nesterenko B, Perfetti P, LeLay G and Sebenne C 1996 *J. Vac. Sci. Technol.* A **14** 2448
[9] Kim N D, Kim Y K, Park C-Y, Yeom H W, Koh H, Rotenberg E and Ahn J R 2007 *Phys. Rev.* B **75** 125309
[10] Sakamoto K, Setvin M, Mawatari K, Eriksson P E J, Miki K and Uhrberg R I G 2009 *Phys. Rev.* B **79** 045304
[11] Battaglia C, Gaál-Nagy K, Monney C, Didiot C, Schwier E F, Garnier M G, Onida G and Aebi P 2009 *J. Phys.: Condens. Matter* **21** 013001
[12] Wei J, Williams E D and Park R L 1991 *Surf. Sci. Lett.* **250** L368
[13] Olshanetsky B Z, Teys S A and Kozhemyako I G 1998 *Phys. Low-Dimens. Struct.* **11/12** 85
[14] Gai Z, Zhao R G, Sakurai T and Yang W S 2001 *Phys. Rev.* B **63** 085301
[15] Battaglia C, Gaál-Nagy K, Monney C, Didiot C, Schwier E F, Garnier M G, Onida G and Aebi P 2009 *Phys. Rev. Lett.* **102** 066102
[16] An T, Yoshimura M, Ono I and Ueda K 2000 *Phys. Rev.* B **61** 3006
[17] Stekolnikov A A, Furthmüller J and Bechstedt F 2004 *Phys. Rev. Lett.* **93** 136104
[18] Battaglia C, Monney C, Didiot C, Schwier E F, Mariotti M, Garnier M G and Aebi P 2010 *AIP Conf. Proc.* **1199** 5
[19] Battaglia C, Onida G, Gaál-Nagy K and Aebi P 2009 *Phys. Rev.* B **80** 214102
[20] Green M A 1990 *J. Appl. Phys.* **67** 2944